ICMIEE20-154

Numerical Analysis of Wall Characteristics for Turbulent Swirling Jets Impinged on a Concave Surface

Joy Saha, Nahid-Al-Nahian Rahat, Zahir U. Ahmed*
Department of Mechanical Engineering, Khulna University of Engineering & Technology, Khulna-9203, Bangladesh

ABSTRACT
Impingement jets systems provide an effective method for achieving particularly high heat transfer coefficient. Whilst a significant amount of studies are available for flat surfaces, the flow and thermal performance for curved surface is limited in the literature. As such, a numerical study using finite volume method is conducted to investigate the wall behaviors, such as pressure, friction and heat transfer characteristics along the concave surface. In this regard, both non-swirling and swirling jets are considered in the range (S = 0 – 0.72) for a Reynolds number equals to 11,000 at various dimensionless nozzle-to-impingement surface distances ($4.5 \leq H/D \leq 7.5$). The Reynolds-averaged momentum and energy equations are solved together, with turbulence described by a two-equation turbulence model, such as the k-ϵ model. The simulation data is first compared with the literature for non-swirling jets on curved surface and the data agrees with convincing accuracy. The results of this study show the effects of the surface characteristics of non-swirling and swirling jets significantly depend on both the swirl effect and the impingement distance.

Keywords: Impingement jets, Turbulent flow, Heat transfer, Concave surface, Swirling, Non-swirling.

1. Introduction

Impingement jets are used in order to obtain significantly greater heat transfer coefficients rate in various mechanical processes such as cooling of in gas turbine blades, hot steel plates, electronic components, drying of paper and textiles, glass and rocket launcher cooling, annealing of steel and glass etc. The impinging jet can drastically decrease the operational cost by enhancing the efficiency of heating/cooling of the system as well as preventing earlier failures. Furthermore, along with removing high heat fluxes, the effects of different properties such as physical properties of fluid, thickness of the jet, inlet velocity, and outlet zone were analyzed [1]. The circular impinging jets flow topology is renowned; it depends on the diameter of the nozzle and nozzle to surface distance and divided into few fluid characteristic zones, including the flow separation zone. The main limitation is the radial non-uniformity of the jet impingement [2,3]. A high rate of heat and mass transfer rate is required for chemical vapor deposition and electronic cooling. This problem has been solved by the use of swirling impinging jet for getting radial uniformity and high heat transfer rate. Huang and El Genk [4] show by flow visualizations, tangential velocity component characterized swirling impinging jets by broadening impinged area. In early studies, organization of turbulence jet flow has remained as an active field, because of its accurate predictions in the acoustics, mixing and combustion by exhibiting a degree of swirling. In the near area, dynamic features belong to m = 0 and m = 1 oscillations; where m represented the Fourier azimuthal wavenumber [5].

Several studies have been performed from two-dimensional slot air swirling impinging jets nozzle to a concave surface. In past numerical investigated, to get solutions for the constant wall boundary layer by using energy and momentum equations, slot jet impingement on a concave surface was studied by Yang et al. [6] who numerical investigated turbulent flow behavior between curved surfaces and two-dimensional air slot jet with using constant heat flux, and selecting well established $k - \mathcal{E}$ turbulence model and its associated wall function for describing the turbulent surface. By using the second-order Cauchy-Euler equation for getting an analytical solution from the momentum equation, an approach for the cooling of isothermal heated flux surface to solve the energy equation was conducted by Chou and Hung [7]. Geunyoung Yang [8] studied experimentally, semi-circular concave surface with three different slot jets ejected flow with variations of jets exit Reynolds number (Re) including different jet to impingement surface distance and various range of Reynolds number.

Larion et al. [9] experimentally analyzed multi-channel swirling air impinging jets heat transfer rate and uniformity on a flat plate. They were concerned about the influence of the swirl number in helical inserts based on the swirling nozzle, which is impeccable for the industrial environment. Fixing a constant Re (28,000) and changing swirl number with five swirl number S (0, 0.2, 0.4, 0.6, and 0.8) and five measurements of the nozzle to surface

* Corresponding author. Tel.: +88-01786590090
E-mail addresses: joysaha64@gmail.com

distance H (2, 4, 6, 8 and 10 diameters). The showed swirling impinging jets compare with a circular impinging jet in the same environment by obtaining experimental data with several conditions such as slot jets, multi-channel jets, circular jets, weak swirl jet and strong swirl jets. A submerged impinging jet insight into the local heat transfer is presented by Rohlfs et. al [10] where used laminar flow for a range of Reynolds number Re ($392 \leq Re \leq 1804$), including with different inlet profile velocities under axisymmetrical conditions. Here, strong radial acceleration was generated by the uniform velocity profiles leading to the inner peak and the outer peak was get to the large scale vortices, including with the heated wall. A fluctuation of the inlet velocity might generate the influence of large scale vortices and their interaction surface. This numerical simulation of the local flow acceleration was studied with low Reynolds number with Nusselt number radial distribution.

An experimental analysis of a dual swirling flame impinging jets on a flat plate has been performed by Satpal et. al [11] to show the compressed heat transfer characteristic of natural gas (CNG)/air dual flame. The heat transfer characteristics have been appreciated for various invariable effects such as different inner and outer vane swirling angles, Reynolds number (Re = 5000 – 9000), and several nozzles to surface distance. At the curved surface stagnation region, with different swirler angle and nozzle-to-surface distance, there was an analysis of heat transfer characteristics. Finally, they show high average heat transfer to the surface on the flat plate for dual flame. Greco et. al [12] studied experimentally, circular synthetic impinging air jets for several time and phase average heat transfer and flow characteristics in different fluid conditions. For investigated experimentally, constant Reynolds number (Re = 5100) and Strouhal number (0.024) with a varying nozzle to surface distance, an infrared camera (IR) used for heat transfer measurements for both time and phase. Heat transfer enhancement produced by the twin configurations where the jet axes distance 3 to 5 diameters. A steady flow with less turbulent flow behaviour showing over the impingement cooling occurs after the main region and the stagnation region, accurate phase description of the heat transfer procedure.

A numerical studied for the axisymmetric turbulent impinging jets has done by Ahmed et. al [13] where they developed the non-swirling versus swirling impinging jets to understand the effect of inflow characteristics and used Reynolds-Averaged Navier-Stokes (RANS) turbulence model. The inlet swirling velocity profiles, no vortex with constant Reynolds number (Re = 23,000), and weakly swirling jets ($S \leq 0.3$) was used to develop the impinging jets. They performed calculations to compare with swirling and non-swirling impinging jets streamwise development. Owsenek et. al [14] investigated numerically, axial and radial laminar flow impingement jets on a flat surface where they have been analyzed the swirling effect on heat transfer by solving energy equations and Navier-Stokes equations. They observed, superposed swirl into the radial jet and enhanced 77% heat transfer rate by the superimposed swirl number unity. Heat transfer for a circular impinging jet for a turbulent air swirling model were experimentally examined by Ichimiya and Tsukamoto [15]. An inflow-type swirl produced by the process of air inserting for the two exits the circular nozzle, flow visualized by producing smoke and surface temperature measured by thermosensitive crystal liquid. Within the present conditions, the heat transfer for different swirling angels is enhanced.

Huang and El-Genk [16] experimentally studied, heat transfer and flow visualization of swirling and multi-channel impinging jets where they compare performance with conventional impingement jets, for several numbers of diameter with the same conditions. 25.4 mm long impinging jet is attached in the system and air flow divert the exit housing tube with different swirl angle ($\Theta = 15°$, 30° and 45°) and solid inserted by the narrow channel in vertical ($\Theta = 90°$). In multi-channel impinging jet local and average heat transfer were calculated in the process and it was generally higher than the conventional impinging jet. They found the best result for $\Theta = 15°$ and nozzle to surface distance 50.8 mm. For visualizing flow, smoke was used. Wen and Jang [17] presented and discussed the experimental results for the heat transfer in constant heat flux test plate and the impinging jets by the round jets and with/without swirling inserted. The total process was examined by different Reynolds number ($500 \leq Re \leq 27{,}000$) and nozzle to test plate distance from 3 to 16. For investigating the flow behaviour, smoke was used under the swirling flow conditions. Casanova [18] performed numerical simulations of the swirling impinging jets with a heated solid wall at a constant temperature. He proposed to heat transfer coefficients correlations along with the heat wall function for different Reynolds number, swirl intensity and nozzle to surface distance. In the jet velocity profile nozzle exit and mathematical models are exposed by seven Reynolds number and nozzle specifications. Here dimensionless parameters Reynolds number ranging for 7000 to 20000 and different swirling number, and different nozzle to heat surface distance. They presented the result to obtain some proposed correlations.

In the impinging jets, literature reviews analyzed curved surface characteristics with nusselt number for different geometry and different nozzle to surface distance together with steady-state turbulent flow. For the research, changed the geometry with several circumstances with changing inlet diameter and curved surface diameter with different nozzle-to-impinging surface (H/D) distance and adding swirling turbulent flow. Here, overall wall characteristics results will be optimized for finding the best result.

2. Methodology

2.1 Physical Model

The figure 1 diagram illustrates the circular jet impingement curve surface where curve surface radius is (R = 195mm), the inlet circular jet diameter is (D = 40mm), the nozzle-to-impingement surface distance (H = 180mm) with constant heat flux.

2.2 Governing Equations

For solving curved surface forced convective heat transfer problem, the following assumptions are considered:

(1) Two-dimensional turbulence flow,
(2) Incompressible steady-state fluid,
(3) Fluid properties are constant, and
(4) Radiative and natural convective heat transfer are negligible.

To complete the CFD investigation of the impinging jet on curve surface with louvered strip inserts and to describe forced convective heat transfer, continuity, momentum, and energy equations are needed.

(1) Continuity equitation:

$$\frac{\partial u}{\partial x}+\frac{\partial v}{\partial x}=0 \quad (1)$$

(2) Momentum equation:

$$\rho\left(u\frac{\partial u}{\partial x}+v\frac{\partial u}{\partial y}\right)=-\frac{\partial p}{\partial x}+\frac{\partial \tau_{xx}}{\partial x}+\frac{\partial \tau_{yx}}{\partial y} \quad (2)$$

$$\rho\left(u\frac{\partial v}{\partial x}+v\frac{\partial v}{\partial y}\right)=-\frac{\partial p}{\partial y}+\frac{\partial \tau_{xy}}{\partial x}+\frac{\partial \tau_{yy}}{\partial y} \quad (3)$$

(3) Energy equation:

$$\frac{\partial}{\partial x_j}\left(\rho u_j C_p T-k\frac{\partial T}{\partial x_j}\right)=u_j\frac{\partial \rho}{\partial x_j}+\left[\mu\left(\frac{\partial u_i}{\partial x_j}+\frac{\partial u_j}{\partial x_j}\right)-\frac{2}{3}\mu\frac{\partial u_k}{\partial x_k}\delta_{ij}\right] \quad (4)$$

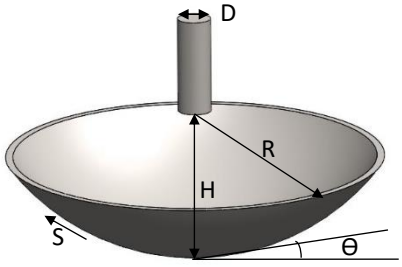

Fig. 1 A schematic of the physical concave surface model.

2.3 Computational Domain

The two-dimensional axis-symmetrical circular air jets that impinge on the inner concave shaped surfaces are made prone to boundary conditions with constant heat flux at the wall with constant inlet fluid temperature, pressure outlet and constant temperature adiabatic wall region. The steady-state incompressible and symmetric about the axis are shown in figure 2(a). The nozzle to impinging surface distance will be changed in different geometry but all similar conditions.

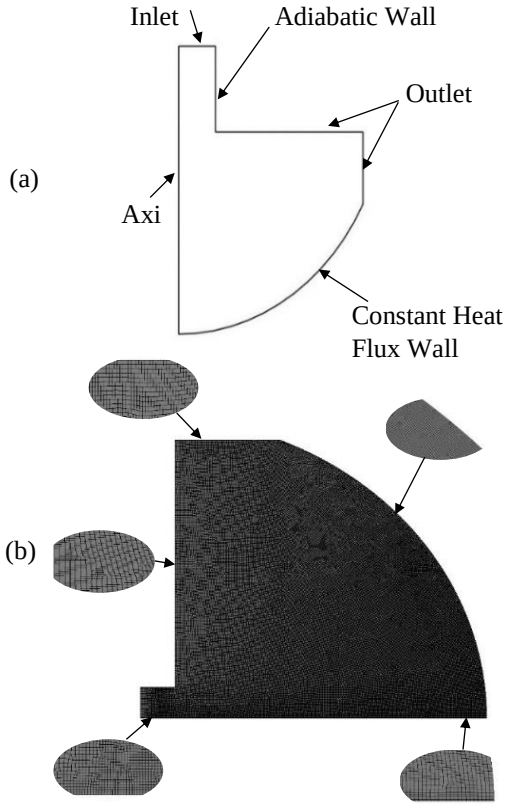

Fig. 2 Solution Domain for the solving numerical problem (a) Computational Domain, (b) Mesh Generation

2.4 Mesh Generation

For solving the numerical problem, mesh is generated by structural way in a number of division methods. Here, the number of divisions is applied to edges by adding several bias factors in the outlet zone. The very structural mesh was built in the surface region. Quadrilateral cell type mesh was created with 66428 nodes, 65852 elements, 0.579 maximum skewness, 0.72668 minimum orthogonal quality, and 1.6715 maximum aspect ratio.

Table 1 Date for Mesh Independency Test

Case	Number of Nodes	Number of Elements	Stagnation Point Nusselt Number
01	53957	53124	119.61
02	59195	58156	122.71
03	63154	62651	123.23
04	66428	65852	125.68
05	68928	67712	125.72

2.5 Boundary and Cell Zone Conditions

The present problem boundary conditions are regulated for the computational domain analysis as shown in fig. 2 (b). The value of heat flux of (5663W/m^2) is

located at the wall curve surface and the inlet jet temperature is (298K).

(1) Inlet Boundary:

$$u = u_{in}, \quad v = 0$$
$$T_j = 25℃ = 298K$$
$$k = \frac{3}{2}\sqrt{u^2 + w^2}$$
$$\omega = \frac{k^{1/2}}{c_\mu^{1/4_l}}$$

(2) Adiabatic Wall:

$$u = v = 0$$
$$\frac{\partial T}{\partial n} = 0$$

(3) Constant heat flux boundary:

$$q^{"} = -k\frac{\partial T}{\partial n}$$

(4) Outlet boundary:

$$p_{ext} = p_{ref} = 1\ atm$$
$$\frac{\partial T}{\partial x} = \frac{\partial k}{\partial x} = \frac{\partial \varepsilon}{\partial x} = 0$$

ANSYS FLUENT 16.2, commercial software was used in the present study to solve the numerical simulation by solving continuity, momentum, and energy equation.
The numerical studies were carried out by both transient and steady method, SST k-ω, where air is the primary fluid. Enhanced wall treatment was used for the turbulence model. The simulation solution method has been set as a simple coupling of pressure velocity, momentum to second-order upwind, fraction of the volume is compressive. Turbulent kinetic energy, momentum, and common rate of dissipation are set upwind in the second order. For the solution control under the relaxation factor is set in pressure 0.3, density 1.0, body forces 1.0, momentum 0.7, turbulent kinetic energy 0.8, specific dissipation rate 0.8, turbulent viscosity 1.0, and energy 1.0. The solution convergence criteria are set as 10^{-6} for normalized residuals of all the algebraic equation. Standard initialization method was chosen in solution initialization. The iteration worked until the convergence conditions were achieved.

3. Result and Discussion

In this study, the numerical simulations are performed by comparing numerical model prognostics with attainable experimental data from a reliable source in the literature review. The impinging jet numerical simulation has been accomplished together with Reynolds number equals to 11000, dimensionless nozzle-to-surface distance H/B (4.5 to 7.5), with constant heat flux q'' (5663 W/m^2).

3.1 Numerical validation

For the numerical simulation theoretical model validation and the suitable boundary conditions, the present studies results have compared to the attainable experimental and numerical result in the literature. Figure 3 indicates the variation of local nusselt number along the constant wall heat flux boundary region. It has been found that the local Nusselt number is comparatively high at the stagnation region and from which it starts decreasing till the very end of the wall. The data of various turbulence models were plotted along a non-dimensional S/D parameter, and these were compared with the simulation data of Yang et al [6]. The behaviour of the variation of local Nu is quite similar to that obtained from the data of Yang et al [6]. It has been seen that standard k-Ɛ and SST k-ω produced better results. SST k-ω turbulent approach was finally considered.

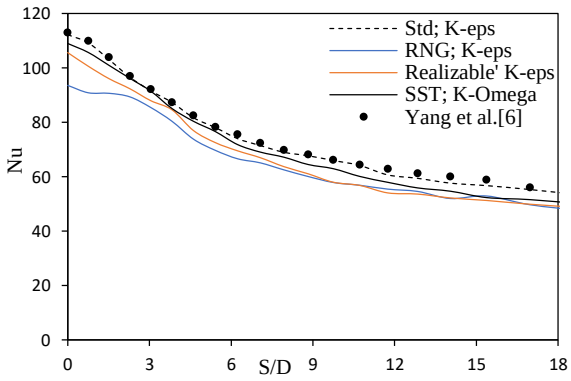

Fig. 3 Local Nusselt number distribution along the curve length (S/D) at H/B=12, B/D= 0.033 and Re= 23700

3.2 Flow characteristics and heat transfer

The axisymmetric turbulence impinging jets have been analyzed. The variation of local and average Nusselt number and heat transfer coefficient with impingement velocity or Reynolds number along the constant wall heat flux was studied and presented here. The effect of swirl number on local Nusselt number can be demonstrated from figure 4. Keeping the Reynolds number constant, it had been found that when no swirling was considered the stagnation point nusselt number was quite high. And at low swirl, the behavior was somewhat similar to no swirl condition i,e Nu was found to be higher near stagnation region which kept on decreasing from that region. However, a different scenario was depicted when considering high swirling jets where it had been observed that the Nusselt was initially low and starts increasing from the stagnation point. It reaches a peak value when S/D is in between 1 to 2, and after that, the local Nusselt number starts diminishing.

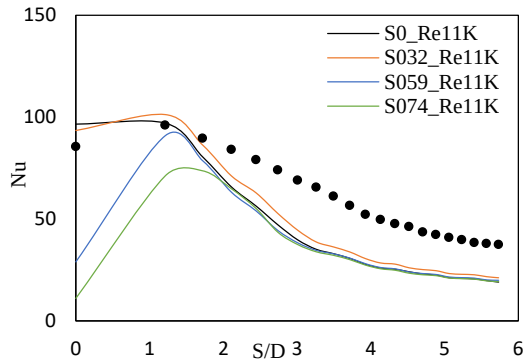

Fig. 4 Local Nusselt number on the impingement wall along with the stagnation point (H/B=4.5, B/D=0.111)

For analyzing the flow characteristics the pressure coefficient graph was included in figure 5. The value of the coefficient of pressure is seen to be higher at the stagnation point and it decreases gradually towards the outlet region. For no swirl and low swirl, there was a sharp drop in the value of pressure coefficient when S/D is in between 0 and 1.5. As for high swirl, a peak in the value of pressure coefficient was not found at the stagnation point but rather to a region near the stagnation point as indicated in the figure 5. Furthermore, a high swirl number corresponded to a lower value of pressure coefficient.

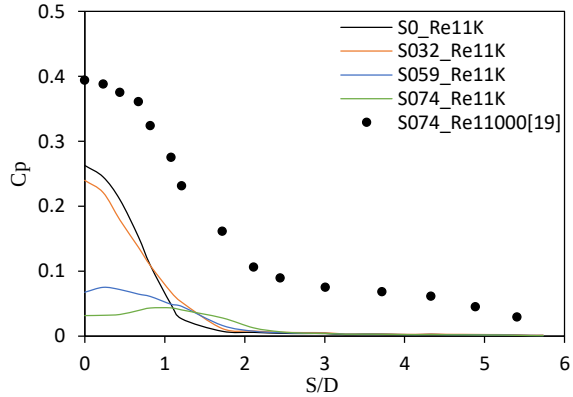

Fig. 5 Coefficient of pressure on the impingement surface along with the stagnation point (H/B=4.5, B/D=0.111)

In all cases, the friction coefficient's value at the stagnation point is the lowest as shown in figure 6. From this point, there is an increase in the value, and after a certain distance it reaches to a peak value and from there a downward slope followed every cases. When the swirl number is low, the peak is more closer to the stagnation point and as the swirl number increases, the peak point moves further away from the stagnation point.

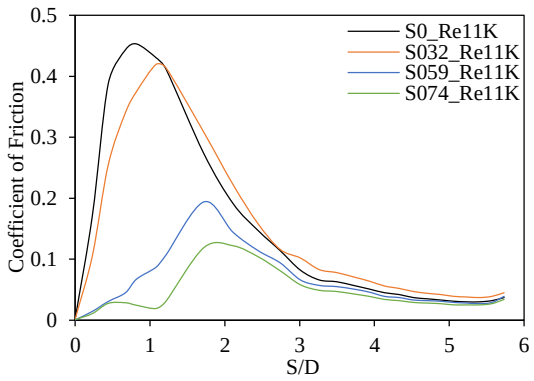

Fig. 6 Coefficient of Friction on the impingement surface along with the stagnation point (H/B=4.5, B/D=0.111)

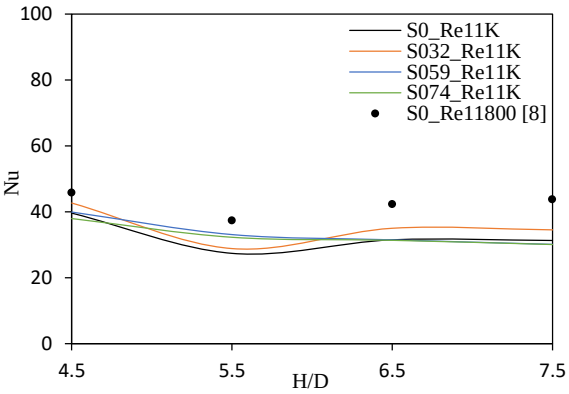

Fig. 7 Average Nusselt Number with different nozzle-to-impinging surface distance

By varying the nozzle-to-impinging surface (H/D), there has been a variation in the average surface Nusselt number which was demonstrated by figure 7. The average Nusselt number is higher when H/D=4.5, the value then slightly diminishes at H/D=5.5 and at a higher nozzle-to-impinging surface distance there is not an appreciable variation in the average surface Nusselt number. The obtained data were compared with Yang et al [8] by increasing the swirling number, the heat transfer co-efficient was enhanced in all nozzle-to-impinging surface (H/D) distance.

Here, showed axisymmetric turbulence impinging jet results where all of those result's graph are presented and compared with a related experimental and numerical graph which are collected from same conditions several papers. By analyzing all graphs we can concluded that, all of those presented graphs are showed very similar behavior with comparing graph.

4. Conclusion

In this research, heat transfer and flow characteristics were numerically investigated for both swirling and non-swirling turbulent impinging jets on a concave surface.

The wall characteristics were explained, for every case 11000 Reynolds number with several swirl numbers were considered. The Reynolds-averaged momentum and energy equations are solved for analyzing the pressure, friction and heat transfer characteristics along the concave surface. Here keeping the constant Reynolds number, decreasing the swirling number the local nusselt number, pressure coefficient, friction coefficient will be increased in the stagnation region and reaches the pick value when S/D between 1 to 2 after that values starts reducing. The average nusselt number was analyzed along with different dimensionless nozzle-to-impinging surface distances.

5. References

[1] Rahman M.M., Dontaraju P., and Ponnappan R., 2002, "Confined jet impingement thermal management using liquid ammonia as the working fluid," In: Proceedings of ASME IMECE2002, November 17-22, New Orleans, Louisiana 33033.

[2] J.W. Gautner, J.N.B. Livingwood, P. Hrycak, Survey of literature of flow characteristics of a single turbulent jet impinging on a flat surface, NASA TN D-5652(1970).

[3] C.D. Donaldson, R.S. Snedeker, A study of free jet impingement. Part 1. Mean properties of free and impinging jets, Journal of Fluid Mechanics 45 (1971) 281-319.

[4] L Huang, M.S. El-Genk, Heat transfer and flow visualization experiments of swirling, multi-channel, and conventional impinging jets, International Journal of Heat and Mass Transfer 41 (1998) 583-600.

[5] Davoust S, Jacquin L, Leclaire B. New results on the structure of turbulence in a mixing layer with and without swirl. Int J Heat Fluid Flow 2014;49:11–7.

[6] Yue-Tzu Yang, Tzu-Chieh Wei, Yi-Hsien Wang, Numerical study of turbulent slot jet impingement cooling on a semi-circular concave surface, Int. J. of Heat and Mass Transfer 54 (2011) 482 – 489.

[7] Y.J. Chou, Y.H. Hung, Impingement cooling of an isothermally heated surface with a confined slot jet ASME, J. Heat Transfer 116 (1994) 479–482.

[8] Geunyoung Yang, Mansoo Choi, Joon Sik Lee, An experimental study of slot jet impingement cooling on concave surface: effects of nozzle configuration and curvature, Int. J. Heat Mass Transfer 42 (1999) 2199–2209.

[9] Ianiro A, Cardone G. Heat transfer rate and uniformity in multi-channel swirling impinging jets. Appl Therm Eng 2011;49(0):89–98.

[10] Rohlfs W, Haustein HD, Garbrecht O, Kneer R Insight into the local heat transfer of a submerged impinging jet: influence of local flow acceleration and vortex-wall interaction. Int J Heat Mass Transf 2012;55(25):7728 – 36.

[11] Singh S, Chander S. Heat transfer characteristic of dual swirling flame impinging on a flat surface. Int. J. Therm Sci 2015:89:1 – 2.

[12] Greco CS, Ianiro A, Cardone G. Time and phase average heat transfer in single and twin circular synthetic impinging air jets. Int J Heat and Mass Transf 2014;73:776 – 88.

[13] Ahmed ZU, Al-Abdeli YM, Matthews MT. The effect of inflow conditions on the development of non-swirling versus swirling impinging turbulent jets. Comput Fluids 2015:118:255-73.

[14] Owsenek BL, Cziesla T, Mitra NK, Biswas G. Numerical investigation of heat transfer in impi-nging axial and radial jets with superimposed swirl. Int J Heat and Mass Transfer 1997;40(1):141–7.

[15] Ichimiya K, Tsukamoto K. Heat transfer from an inflow-type swirling turbulent impinging jet. JSME Int J Ser B Fluids Therm Eng 2006;49(4):995-9.

[16] Huang L, El-Genk MS. Heat transfer and flow visualization experiments of swirling, multi-channel, and conventional impinging jets. Int J Heat Mass Tranf 1998;41(3):583-600.

[17] Wen M, Jang K. An impinging cooling on a flat surface by using circular jet with longitudinal swirling strips. Int J Heat Mass Transf 2003;46(24):4657 – 67.

[18] Ortege-Casanova J. CFD and correlations of the heat transfer form a wall at constant temperature to an impinging swirling jet. Int. J Heat and Mass Transfer 2012:30(3):325-40.

[19] S. Debnath, d.H.U. Khan, Z.U. Ahmed, Turbulent Swirling Impinging Jet Arrays: A Numerical Study on Fluid Flow and Heat Transfer, Thermal Science and Engineering Progress (2020).

NOMENCLATURE

C_p	Pressure Coefficient (dimensionless)
S	Swirl number (dimensionless)
D	Nozzle Diameter (m)
R	Concave surface radius
H	Nozzle to plate distance
Re	Reynolds number (dimensionless)
k	Turbulent kinetic energy (m^2/s^2)
ω	Specific rate of dissipation
Nu	Nusselt number (hD/k)
v	Axial mean velocity (m/s)
u	Bulk axial velocity (m/s)
x	Axial co-ordinate (m)
y, z	Cartesian coordinates (m)